

A METALLURGICAL ANALYSIS OF AN ASTM
A 212-B STEEL TANK CAR HEAD PLATE

J. G. EARLY

NATIONAL BUREAU OF STANDARDS
WASHINGTON, DC 20545



APRIL 1981
FINAL REPORT

Document is available to the public through the
National Technical Information Service,
Springfield, Virginia 22161.

Prepared for
U.S. DEPARTMENT OF TRANSPORTATION
FEDERAL RAILROAD ADMINISTRATION
Office of Research and Development
Washington, D.C. 20590

NOTICE

This document is disseminated under the sponsorship of the Department of Transportation in the interest of information exchange. The United States Government assumes no liability for its contents or use thereof.

NOTICE

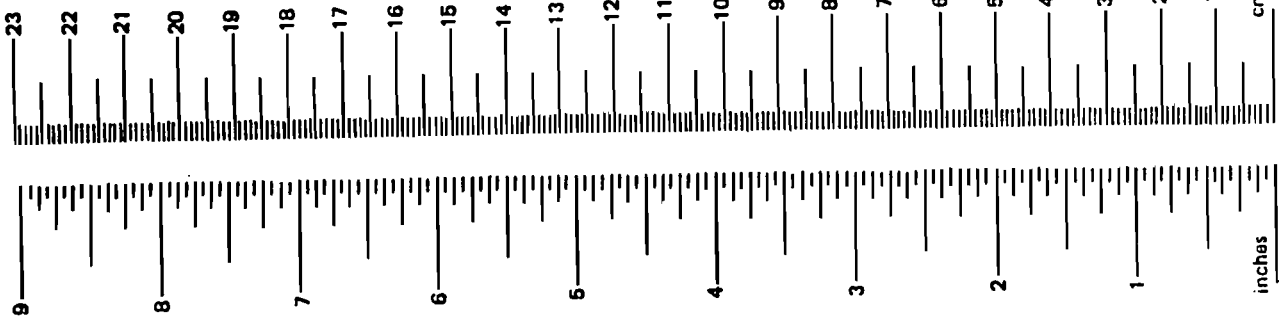
The United States Government does not endorse products or manufacturers. Trade or manufacturers' names appear herein solely because they are considered essential to the object of this report.

1. Report No. FRA/ORD-81/32		2. Government Accession No.		3. Recipient's Catalog No.	
4. Title and Subtitle A METALLURGICAL ANALYSIS OF AN ASTM A212B STEEL TANK CAR HEAD PLATE				5. Report Date April 1981	
				6. Performing Organization Code	
7. Author(s) J. G. Early				8. Performing Organization Report No. NBSIR 78-1582	
9. Performing Organization Name and Address National Bureau of Standards Washington, DC 20234				10. Work Unit No. (TRAIS)	
				11. Contract or Grant No. AR-4008	
12. Sponsoring Agency Name and Address U.S. Department of Transportation Federal Railroad Administration Office of Research and Development Washington, DC 20590				13. Type of Report and Period Covered Final Report	
				14. Sponsoring Agency Code	
15. Supplementary Notes					
16. Abstract <p>The sample was taken from the A-head plate of tank car SOEX 3033 involved in an accident near Winder, Georgia. The A-head plate was reportedly produced to specification ASTM A212-65, Grade B steel. The results of laboratory check chemical analyses indicated that the plate sample met the chemical requirements of ASTM A212-65, Grade B steel. The results of ambient-temperature bend tests and tensile tests showed that the plate sample satisfied both the bend requirements and the tensile elongation requirements but failed to meet the minimum ultimate tensile strength and yield point requirements of ASTM A212-65, Grade B steel. The results of metallographic analyses revealed substantial variation in the microstructure in the plate thickness direction. The observed coarse prior austenite grain size and large ferrite grain size is consistent with the coarse-grain steelmaking practice allowed for ASTM A212 steel and a high finishing temperature during fabrication. Hardness measurements of the microstructure correlated well with the measured tensile strength properties. The nil-ductility transition temperature was determined to be 30 F, a value equal to the highest value reported for a group of tank car plate samples, including both accident samples and current and previously allowed tank car plate materials. The results of Charpy V-notch tests established that the 15 ft-lb energy absorption and 50% shear fracture appearance transition temperatures measured for both longitudinal and transverse specimens were all above 60F and within normal tank car service temperature range. The high transition temperatures are related to both the coarse prior austenite grain size and large ferrite grain size observed in the microstructure and the steel chemistry.</p>					
17. Key Words Impact Properties Rail Tank Cars Pressure Vessels			18. Distribution Statement Document is available to the public through the National Technical Information Service, Springfield, Virginia 22161		
19. Security Classif. (of this report) Unclassified		20. Security Classif. (of this page) Unclassified		21. No. of Pages	22. Price

METRIC CONVERSION FACTORS

Approximate Conversions to Metric Measures		Approximate Conversions from Metric Measures	
Symbol	When You Know	Multiply by	To Find
LENGTH			
in	inches	2.5	centimeters
ft	feet	30	centimeters
yd	yards	0.9	meters
mi	miles	1.6	kilometers
AREA			
in ²	square inches	6.5	square centimeters
ft ²	square feet	0.09	square meters
yd ²	square yards	0.8	square meters
mi ²	square miles	2.6	square kilometers
	acres	0.4	hectares
MASS (weight)			
oz	ounces	28	grams
lb	pounds	0.45	kilograms
	short tons (2000 lb)	0.9	tonnes
VOLUME			
tsp	teaspoons	5	milliliters
Tbsp	tablespoons	15	milliliters
fl oz	fluid ounces	30	milliliters
c	cups	0.24	liters
pt	pints	0.47	liters
qt	quarts	0.95	liters
gal	gallons	3.8	liters
ft ³	cubic feet	0.03	cubic meters
yd ³	cubic yards	0.76	cubic meters
TEMPERATURE (exact)			
°F	Fahrenheit temperature	5/9 (after subtracting 32)	Celsius temperature
°C	Celsius temperature	9/5 (then add 32)	Fahrenheit temperature

*1 in. = 2.54 cm (exactly). For other exact conversions and more detail tables see NBS Misc. Publ. 286, Units of Weight and Measures. Price \$2.25 SD Catalog No. C13 10 286.



Symbol	When You Know	Multiply by	To Find
LENGTH			
mm	millimeters	0.04	inches
cm	centimeters	0.4	inches
m	meters	3.3	feet
m	meters	1.1	yards
km	kilometers	0.6	miles
AREA			
cm ²	square centimeters	0.16	square inches
m ²	square meters	1.2	square yards
km ²	square kilometers	0.4	square miles
ha	hectares (10,000 m ²)	2.5	acres
MASS (weight)			
g	grams	0.035	ounces
kg	kilograms	2.2	pounds
t	tonnes (1000 kg)	1.1	short tons
VOLUME			
ml	milliliters	0.03	fluid ounces
l	liters	2.1	pints
l	liters	1.06	quarts
l	liters	0.26	gallons
m ³	cubic meters	36	cubic feet
m ³	cubic meters	1.3	cubic yards
TEMPERATURE (exact)			
°C	Celsius temperature	9/5 (then add 32)	Fahrenheit temperature

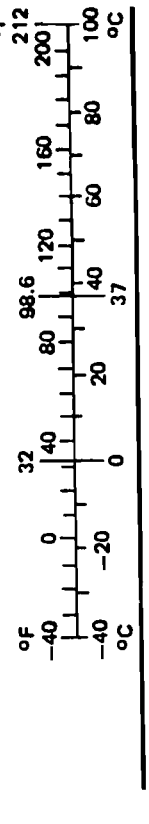


Table of Contents

	<u>Page</u>
1. INTRODUCTION.....	1
2. PURPOSE.....	2
3. EXPERIMENTAL PROCEDURES.....	2
3.1 Macroscopic Observations and Rolling Direction Determination.....	2
3.2 Chemical Analysis.....	2
3.3 Tensile Testing.....	2
3.4 Bend Testing.....	3
3.5 Impact Testing.....	3
3.6 Metallographic Studies and Hardness Testing.....	4
4. RESULTS AND DISCUSSION.....	4
4.1 Chemical Composition.....	4
4.2 Macroscopic Observations.....	5
4.3 Metallographic Analysis.....	5
4.4 Hardness Measurements.....	6
4.5 Tensile Properties.....	6
4.6 Bend Behavior.....	8
4.7 Inclusion Content.....	8
4.8 Impact Properties.....	9
4.8.1 Nil-Ductility Transition Temperature.....	9
4.8.2 Charpy V-notch Tests.....	9
4.9 General Discussion.....	11

Table of Contents (continued)

	<u>Page</u>
5. CONCLUSIONS.....	13
6. ACKNOWLEDGEMENT.....	14
REFERENCES.....	15

TABLES

- I. Chemical Composition of the Winder Sample
- II. Tensile Properties of the Winder Sample
- III. Bend Behavior of Winder Sample
- IV. QTM Inclusion Content Rating of Winder Sample
- V. Drop-Weight Test Behavior of Winder Plate
- VI. Charpy V-notch Impact Transition Temperatures for Four Head Plate Steels Tested at NBS
- VII. Comparison of Charpy V-notch Upper-Shelf Behavior of Four Head Plates Tested at NBS
- VIII. Comparison of Selected Results From Check Chemical Analyses of Four Head Plates Tested at NBS

FIGURES

1. Photograph of Tank Car SOEX 3033 at Accident Site Near Winder, GA.
2. Close-up of A-Head, Tank Car SOEX 3033
3. Winder Plate Sample
4. Winder Plate Sample Showing Location and Orientation of Test Specimens
5. Schematic Shwoing Planes Associated With the Rolling Direction in a Plate
6. Representative Photomicrographs of Inclusions on Two Orthogonal Planes

FIGURES (continued)

7. Montage of Microstructure Through Cross-Section of the Plate
8. Photomicrographs of Typical Microstructure from Zones 2 and 3
9. Representative Photomicrographs of a Section Through a Transverse Tensile Specimen
10. Bend Test Specimens
11. Drop-Weight Test Specimens
12. Charpy V-notch Impact Test Results for Head Plate Specimens Taken From ASTM A212 Steel Plate
13. Fracture Appearance of Selected Charpy Specimens

APPENDIX A - Charpy Impact Test Results

Table A1. Energy Absorption for LT Orientation

Table A2. Lateral Expansion for LT Orientation

Table A3. Shear Fracture Appearance for LT Orientation

Table A4. Energy Absorption for TL Orientation

Table A5. Lateral Expansion for TL Orientation

Table A6. Shear Fracture Appearance for TL Orientation



1. INTRODUCTION

A metallurgical evaluation of a steel plate sample (Winder sample) was requested by the Federal Railroad Administration, Department of Transportation. The Winder plate sample was reported [1]^(a) to have been taken from a tank car identified as SOEX 3033 involved in an accident on the Seaboard Coast Line Railroad at approximately 5:25 a.m. on April 6, 1975 near Winder, Georgia. The tank car carrying liquified petroleum gas (LPG), was punctured in the tank head and propelled by the expansion of the liquified gas a distance of about 450 feet from the derailment site. As the tank car rocketed away from the accident site, it apparently struck the asphalt pavement of a nearby highway creating sparks which ignited the LPG vapor. The fracture surfaces near the original impact site on this plate were reportedly perpendicular to the plate surfaces with no evidence of plate thinning at the fracture edge and the mode of failure propagation was stated to be brittle. The ambient temperature at the accident site was estimated to have been about 40 F.

The A-head of the tank car, photographed at the accident site [2] and shown in Figure 1, contained the Winder sample submitted to the National Bureau of Standards (NBS) for metallurgical evaluation. The Winder plate sample was reported to have been cut from an undeformed region of the A-head, as shown in Figure 2. The head plate material used in the fabrication of the A-head was reported [1] to have been produced to the specification for ASTM A-212, Grade B, F.Q. steel.

It should be noted that the test specimens taken from the Winder plate sample for this investigation were in the as-rolled, cold-worked, and stress-relieved condition. The cold work resulted primarily from the original fabrication of the tank-car head and possibly from some slight, but indeterminate amount of reforming during the puncture of the tank car. However, the shape and appearance of the Winder plate sample indicated that negligible reforming occurred in this sample. It is therefore believed that the observations and properties reported in this metallurgical evaluation of the head plate are relevant to the A-head plate of the tank car in service.

2. PURPOSE

The principal purpose of this metallurgical evaluation was to determine if the Winder head-plate sample, taken from tank car SOEX 3033, conformed with the specification ASTM A212-65 for high-tensile strength, carbon-silicon steel plates for pressure vessels, and to determine the impact test behavior of this plate sample.

(a) The isolated numbers in brackets refer to references listed at the end of this report.

3. EXPERIMENTAL PROCEDURES

The orientation of the Winder plate sample with respect to the principal rolling direction of the plate was determined, prior to the preparation of test specimens, by an examination of inclusion morphology.

Chemical analyses, tensile properties and bend characteristics were determined and compared with the requirements of ASTM A212-65. In addition to the required tests, standard Charpy V-notch impact tests, drop-weight nil-ductility transition temperature tests, inclusion content ratings and a hardness survey were performed and macroscopic and microscopic observations were made.

The results of pre-cracked Charpy V-notch impact tests and dynamic-tear tests will be reported in a subsequent report.

3.1 Macroscopic Observations and Rolling Direction Determination

The Winder plate sample was macroscopically examined for evidence of both deformation resulting from the accident and heating effects resulting from the burning LPG. The principal rolling direction was determined using a quantitative television microscope (QTM) by measuring inclusion lengths on a series of specimens oriented at fixed angles with respect to an arbitrary reference line scribed on the plate surface (Figure 3). The location and orientation of test specimens taken from the Winder plate are shown in Figure 4. The longitudinal axes of the longitudinal and transverse specimens are aligned respectively, parallel and perpendicular to the principal plate rolling direction.

3.2 Chemical Analysis

Check chemical analyses (by combustion-conductometric and emission spectroscopy) were conducted by a commercial testing laboratory at the quarter-thickness position of the chemistry sample (Figure 3) to determine if the composition satisfied the requirements of ASTM A212-65, Grade B steel.

3.3 Tensile Testing

Two longitudinal and two transverse specimens, 0.250 inches in diameter with a 1-inch-gage length, were taken as closely as possible from the quarter-thickness position of the plate and tested in accordance with ASTM A370-73, (b) Mechanical Testing of Steel Products.

(b) The General Conditions for Delivery section of the specification for ASTM A212-65 tank-car steel requires that materials furnished to these specifications conform to the applicable requirements of ASTM Specification A20-65. Specification A20-65 requires for plates 1-1/2 inch and under in thickness, tension test specimens shall be Standard Rectangular Tension Test Specimens with 8-inch-gage length and for plates over 1-1/2 inches in thickness, tension test specimens shall be Standard Round Tension Test Specimens with 2-inch-gage length, 0.505 inches in diameter. However, ASTM A20-65 requires the tests be conducted in accordance with the ASTM Methods and Definitions A370, for the Mechanical Testing of Steel

3.4 Bend Testing

Two bend-test specimens, one longitudinal and one transverse, were prepared with dimensions 3/8 inch thick x 1-1/2 inch wide^(c) x 6 inches long and with the outside surface of the tank car being the outer curve of the bend. In accordance with ASTM A212-65 and ASTM A370-73, the specimens were bent through an inside diameter of 3/4 inches, so as to provide the required bend ratio of bend diameter (d) to thickness (t) equal to 2.

3.5 Impact Testing

The results of two types of impact tests are given in this report: drop-weight nil-ductility transition temperature (NDTT) tests, carried out in accordance with ASTM E208-69, and standard Charpy V-notch (CVN) tests, carried out in accordance with ASTM E23-72. Specimens for the NDTT tests were full-plate-thickness type specimens with length and width dimensions of 5 inches and 2 inches, respectively, and a saw-cut notch located on a weld bead on the outside plate surface. The Charpy specimens were standard size and were machined from the quarter thickness location of the plate.

The drop-weight test was originally developed to study the initiation of brittle fractures in low and intermediate structural steels. The test

(b) Cont.

Products. ASTM A370-73 allows Standard Round Tension Test Specimens and Small Size Specimens proportional to the Standard Round Specimen to be used when it is necessary to test material from which the Standard Rectangular Test Specimens of 8-inch- and 2-inch-gage length cannot be prepared. Because the amount of plate material available for machining test samples was limited, it would not have been feasible to prepare the Standard Rectangular Tension Specimens. The Standard Round Tension Test Specimen, 0.505 inches in diameter, has a 2-inch-gage length, thus allowing direct comparison between test result and specification; however, the threaded end section requires a diameter of 3/4 inches and due to the head-plate curvature the plate thickness was insufficient. Thus, for test consistency, the tensile test specimens were machined to standard 0.250-inch-diameter round test specimens with a 1-inch-gage length.

(c) The width of the bend specimens significantly affects the bend ductility. Dieter⁽³⁾ has reported that ductility, in terms of the bend angle before cracking occurs in a material in bending, decreases with increasing values of the width to thickness ratio, w/t, until a terminal level is achieved at a w/t equal to about 8. As this ratio of w/t increases, the ratio of the transverse stress to the circumferential stress also increases and the bend ductility of the specimen decreases. Therefore, in order to have a bend test specimen of "intermediate" severity, the w/t ratio of 4 was chosen for the bend specimens tested at NBS.

is used to measure the nil-ductility transition (NDT) temperature (the temperature above which many steels undergo a transition from brittle to ductile fracture behavior) and permits the evaluation of the ability of a steel to resist crack propagation under yield point loading in the presence of a small flaw. The NDT temperature is independent of the specimen orientation with respect to the plate rolling direction.

The LT and TL specimens used in this study are the standard longitudinal and transverse orientations used in previous reports [4-7]. For all sets of impact specimens, tests were conducted over a temperature range selected to show the transition from ductile to brittle fracture.

3.6 Metallographic Studies and Hardness Testing

Representative photomicrographs, oriented as shown in Figure 5, were obtained on metallographic samples located as shown in Figure 3. Metallographic observations were made on selected polished and etched areas of longitudinal C planes and transverse B planes. The ferrite grain size was measured in accordance with ASTM E112-74, Intercept Method.

Rockwell B hardness measurements were taken on a specimen adjacent to the metallographic specimens and correlated with the microstructure.

The inclusion content was determined on longitudinal C planes by a QTM method which rates the inclusion content as an area percent of the section being rated. The area percentage measurements were made at two quarter thickness locations and at the mid thickness. In addition, the worst field and the number of fields with inclusion area greater than 0.5 percent, were tabulated. In general, the QTM methods described in the literature [5,8] were used.

4. RESULTS AND DISCUSSION

4.1 Chemical Composition

The chemical composition, as determined by the check analysis of the plate sample, is given in Table I, along with the chemical requirements of ASTM A212-65, Grade B steel. The results of the check analysis indicates that the composition of the Winder sample satisfies the chemical requirements for ASTM A212-65, Grade B steel. It should be noted, however, that the carbon and manganese levels are 22 percent and 19 percent, respectively, below the maximum level allowed for this grade of steel.

Specification A212-65 allows either coarse-or fine-grain steelmaking practice for plates of less than two inches in thickness and the lack of detectable amounts of vanadium and aluminum reported in the check analysis indicated that a coarse-grain steelmaking practice was followed. The same deoxidation practice was apparently followed for the previous ASTM A212-B head plate tested at NBS [4].

4.2 Macroscopic Observations

The appearance of the Winder plate sample was compared with a series of photographs taken of the tank car at the accident site. Almost all of the external plate surface of the sample was covered with paint except near the torch-cut edges and in regions containing several scratches and gouges. The appearance of this surface coating was taken as evidence that the region of the tank-car head from which the NBS sample was removed did not experience any significant heating as a result of the fire following the accident. A comparison between Figure 1 and Figures 2 and 3 shows that several of the gouges occurred after the accident and probably resulted during the removal of the tank car from its resting site. Further, the specimen layout (Figure 4) was chosen to avoid most of the gouged areas. Therefore, the results of this study are believed to represent the as-fabricated head plate.

4.3 Metallographic Analysis

Representative photomicrographs taken at low magnification on longitudinal C planes and transverse B planes are shown in the unetched condition in Figure 6. The large difference in inclusion length between the longitudinal and transverse planes indicates that this head plate was not extensively cross-rolled prior to the forming operation.

Representative microstructures are shown in the etched condition in Figures 7 and 8. The microstructure consists of large pearlite colonies and ferrite grains with little evidence of banding and is similar to that reported for another head-plate sample of ASTM A212-B steel [4]. In the present plate, however, there is a high degree of variability from plate surface to plate surface. A montage of the longitudinal plane (Figure 7) microstructure from plate surface to plate surface reveals three distinct zones.

The first zone (Zone 1) consists of a narrow decarburized layer, about 0.02 inches thick, located at both the inside and outside plate surface. The presence of the decarburized layer at both plate surfaces indicates that decarburization probably occurred during the plate rolling and forming operations and/or the stress-relieving operation after fabrication of the tank car.

Proceeding inward from both plate surfaces, the second zone (Zone 2), about 0.19 inches thick, contains large pearlite colonies within which are found acicular or Widmanstätten side plates of ferrite. The pearlite colonies are observed to be generally surrounded by proeutectoid ferrite located on the prior austenite grain boundaries, as shown in Figure 8a.

The third zone (Zone 3), a large region about 0.37 inches thick centered about the plate mid-thickness location, contains a large amount of proeutectoid ferrite which generally masks the prior austenite grain boundaries, as shown in Figure 8b.

The determination of the prior austenite grain size was made possible because of the outline of ferrite located at the prior austenite grain boundaries. The prior austenite grain size was estimated to be ASTM No. 1-2 through comparison with Plate I grain size charts from ASTM E 112. The ferrite grain size of the non-Widmanstatten ferrite grains was ASTM No. 7.1 as determined by the circular intercept method from ASTM E 112. The coarse prior austenite grain sizes found in both the Winder plate sample and the other ASTM A212-B head-plate sample previously studied at NBS are consistent with the conclusions that both steels were produced to coarse-grain practice. ^(d) A coarse austenite grain size will promote the formation of Widmanstatten ferrite in steel containing less than 0.3-0.4 percent-by-weight carbon [9], as seen in Figures 7 and 8.

The symmetry of the microstructural zones (Figure 7) about the plate midthickness location is related to thermal and mechanical effects during processing of the plate because the prior austenite grain size and the cooling rate can affect the relative amounts, grain sizes, and distributions of ferrite and pearlite in these low-carbon steels. [10] Large pearlite colonies and a coarse ferrite grain size are two of the factors which promote high impact transition temperatures.

4.4 Hardness Measurements

The results of hardness measurements are given in Figure 7. The Rockwell B hardness is highly variable, ranging from 73 to 79, and can be correlated with the microstructure. The region of highest hardness, HRB 77 to 79, corresponds to Zone 2 which exhibits the highest proportion of the relatively hard pearlite phase. The region of lowest hardness, excluding the decarburized layer, corresponds to Zone 3, which consists of extensive areas of the relatively soft ferrite phase.

4.5 Tensile Properties

The tensile properties of the Winder sample are given in Table II along with the requirements of ASTM A212-B-65. The results of the longitudinal and transverse specimens indicate that the steel meets the minimum elongation requirement of 21 percent but does not meet the minimum ultimate tensile strength or yield-point requirements of 70 ksi and 38 ksi, respectively.

The average values of longitudinal and transverse ultimate tensile strength were 67.9 ksi and 67.6 ksi, respectively, while the average 0.2 percent offset yield-strength values were 33.0 ksi and 32.2 ksi,

(d) Although the final austenite grain size of hot-worked products is strongly influenced by the finishing temperature of the working operation, steels produced to fine-grain practice resist grain coarsening over a large range of finishing temperatures. Ferrite grain size and pearlite colony size are strongly influenced by the prior austenite grain size and by the cooling rate through the transformation temperature, and are therefore affected by deoxidation practice and finishing temperatures.

respectively. These values indicate that there was little anisotropy in the strength of the plate in the plane of the rolling direction; a finding consistent with earlier results on both head and shell plates of ASTM A212 and AAR M128 steel. [12,13]

Further evidence that the mechanical behavior of this plate sample was not affected by the accident can be found in the measured strength properties. The possible exposure to fire and plastic deformation could lead to strain aging of the plate which can manifest itself by the presence of a sharp yield point, increases in ultimate tensile strength and yield strength, and an increase in the ductile-to-brittle transition temperature, such as measured by Charpy V-notch impact tests. The strength properties, such as ultimate tensile strength and yield strength, of ferritic steels such as ASTM A212-B are determined primarily by the chemical composition, especially the amounts of carbon and manganese. The measured ultimate-tensile-strength and yield-strength values of the Winder sample are below specification minimum requirements. This is consistent with the lower carbon and manganese levels found by the check chemical analysis. Further, the presence of a sharp yield point in three of the four tensile test specimens (see Table II) indicates that any plastic deformation received by the plate sample as a result of the accident was insufficient to eliminate the sharp yield point. Thus the measured strength properties indicate that little or no strain aging occurred as a result of the accident.

The average tensile ductility values, measured by percent elongation, were 37.4 percent and 35.8 percent respectively for longitudinal and transverse specimens. The longitudinal elongation values were approximately four percent higher than the transverse values. This finding is in agreement with the general observation that the tensile ductility of rolled steel plates tends to be greater in the longitudinal direction than in the transverse direction.

Reduction-in-area requirements are not specified in ASTM A212-B-65, but they provide a useful check of the elongation results since percent reduction-in-area measurements are independent of the gage length of the specimen. The trend for the reduction-in-area data given in Table II is similar to those for the elongation data.

The ultimate tensile strength data is consistent with the hardness measurements and the results of the metallographic analyses. Using an empirical relation between hardness and tensile strength [11], the measured hardness range of HRB 73 to 79 would correspond to an ultimate tensile strength range of 64 ksi to 71 ksi, respectively. A photomicrograph of the cross-section of a transverse tensile specimen (shown in Figure 9) points out some of the same microstructural variability as shown across the whole plate thickness in Figure 7. The microstructure of the gage length region (Figure 9b) encompasses the transition region between zones 2 and 3 with a hardness range of approximately 74 to 77. This hardness range corresponds to a range in ultimate tensile strength of 65 ksi to 69 ksi, respectively. The measured average ultimate tensile strength of almost 68 ksi for both longitudinal and transverse specimens falls within this predicted range.

The variation in hardness through the plate thickness will result in a similar variation in mechanical properties. Using the hardness-ultimate tensile strength correlation, only that portion of the plate containing the Zone 2 microstructure would be expected to meet the minimum ultimate tensile strength requirement of ASTM A212-B-65. Hence, the plate clearly does not meet the required minimum tensile strength of ASTM A212-B steel.

4.6 Bend Behavior

The results of the bend tests are given in Table III. Both the longitudinal and transverse specimens, shown in Figure 10, are judged to have passed the requirement of ASTM A212-B-65. There was no evidence of cracking or surface crazing on either of the specimens tested.

4.7 Inclusion Content

The results of the inclusion content rating are given in Table IV. The QTM area-percentage rating at an effective magnification^(e) of X100 indicates that the Winder plate sample had an overall average inclusion content of 0.29 area percent (based on 100 fields). The observed number of fields with an inclusion area equal to or greater than 0.5 percent was found to be six. These results indicate that the Winder sample is cleaner in comparison with the previously reported results for AAR M128-B steel [12].

The results of an earlier QTM inclusion analysis^(f) of head and shell plates of ASTM A212-B steel [4] showed average overall inclusion contents of 0.19 and 0.13 area percent respectively. The observed number of fields with inclusion areas equal to or greater than 0.5 percent were two and zero respectively, for the head and shell plates. Thus the inclusion content rating results show that these two examples of ASTM A212-B steel were similar to each other and cleaner than the Winder head plate.

A further comparison can be drawn between the Winder results and values reported^(g) for larger billet specimens from steel with a broad range of strength levels [8]. The average inclusion area percent range reported was 0.10 to 0.38. The reported range for number of fields with inclusion areas equal to or greater than 0.5 percent was 1 to 26. The Winder plate sample lies between the middle and low ends of these ranges.

(e) The effective magnification of the QTM system represents the actual magnification of the image used by the internal electronic measuring scale of the instrument. The image magnification or apparent magnification, as measured on the visual display monitor, has no meaning because the monitor is not part of the measuring system.

(f) These QTM measurements were reported for an apparent magnification of X338. This is equivalent to an effective magnification of X120 for the particular instrument used.

(g) The reported data were obtained at an apparent magnification of X350 which was equivalent to an effective magnification of X100.

4.8 Impact Properties

4.8.1 Nil-Ductility Transition Temperature

The results of the drop-weight tests are given in Table V. Inspection of the test specimens (pictured in Figure 11) shows that in both specimens tested at +40 F, the weld starter crack did not propagate to either edge of the specimen surface. At 30 F and below, the weld starter crack propagated to at least one edge of the specimen surface. According to the test criteria of ASTM E208-69, the nil-ductility transition temperature is +30 F.

A recent review of fracture toughness properties [14] from selected tank car accident samples as well as from both current and previously allowed tank-car materials (including A212-B steel) reported +30 F as the highest measured nil-ductility transition temperature. Thus, the value of +30 F for the Winder sample is equal to the highest value reported for this group of tank-car plates. This was observed despite the relatively low carbon content and strength of this plate, both of which promote lower transition temperatures.

4.8.2 Charpy V-notch Tests

The results of the Charpy V-notch impact tests on both longitudinal and transverse specimens are given in Figure 12. Experimentally measured values and the calculated curves are both shown for three fracture criteria: energy absorption, percent shear fracture appearance, and lateral expansion. The raw data and the results of calculations for the three plots are given in Appendix A, Tables A1 through A6. The longitudinal (LT orientation) and transverse (TL orientation) specimens are oriented with the specimen axis parallel and perpendicular, respectively, to the principal plate rolling direction.

The results indicate that at temperatures between approximately 180 F and the highest test temperature of 260 F, there is little variation in the observed behavior of either the longitudinal or transverse specimens. In this upper-shelf region, the percent-shear-fracture appearance, energy absorption, and lateral expansion are at a maximum. For the transverse specimens, however, the upper-shelf energy absorption is only two thirds that of the longitudinal specimens, 45 ft-lbs versus 72 ft-lbs, respectively. This reduced performance of the transverse specimens is further reflected in a lower lateral expansion value of 54 mils compared to 72 mils for longitudinal specimens.

At temperatures below about 180 F, the fracture of Charpy specimens is associated with decreasing amounts of energy absorption, percent-shear-fracture appearance, and lateral expansion with decreasing temperature until at some lower temperature all three criteria reach a minimum level called the lower shelf. At temperatures between the upper shelf and the lower shelf, there is a transition zone.

The results indicate that for each of the fracture criteria, the transition zone lies in approximately the same range of temperature, a range of 200 F between -20 F and +180 F. At temperatures below about 100 F, the value of the fracture criteria are independent of specimen orientation while at all higher test temperatures the energy-absorption and lateral-expansion values are greater for the longitudinal specimens.

Photographs of selected fractured Charpy specimens are shown in Figure 13. At temperatures above 40 F where shear fracture appearance was about 15 percent or more, the fracture surfaces of both longitudinal and transverse specimens were similar and contained regions of cleavage fracture, fibrous fracture, and shear lips. Even at 260 F, the highest test temperature used, both longitudinal specimens and transverse specimens contained a slight trace of cleavage fracture, even though the energy absorption and lateral expansion data indicated that the test temperature was within the upper-shelf regime. Generally, the size of the shear lips increased with increasing test temperature, and at a fixed temperature, were larger for longitudinal specimens than for transverse specimens.

Studies of shear fracture appearance from fractured Charpy specimens taken from ASTM A212-B and AAR M128 steel shell plates [4,5] revealed that both longitudinal specimens and transverse specimens exhibited a large scale lamellar fracture appearance. This lamellar appearance was not present in specimens of either orientation from an ASTM A212-B head plate [4] previously studied. Fractured Charpy specimens from the Winder ASTM A212-B head plate, shown in Figure 13, do not contain the massive lamellar appearance, in agreement with the previous observations for an ASTM A212-B head plate.

The Charpy V-notch transition temperatures for longitudinal and transverse specimens for the four head plates tested at NBS [7] are given in Table VI for three commonly reported fracture criteria: 15 ft-lb energy absorption, 15 mil lateral expansion, and 50 percent shear fracture appearance. The ASTM A212-B plates have the highest transition temperatures in the group with the Winder plate having the second highest values. The 15 ft-lb energy absorption and 50 percent shear-fracture-appearance transition temperatures for the Winder sample are all above 60 F and within the normal service temperature range for tank cars. The absence of observed strain-aging effects suggests that the high transition temperatures of the Winder plate sample probably result from effects due to chemical composition and grain size.

The extent of anisotropy resulting from cross-rolling of plate materials can be assessed by the anisotropy index [7], defined as the ratio of the maximum shelf energy of transverse specimens of TL orientation to the maximum shelf energy of longitudinal specimens of LT orientation. Using this relationship, an isotropic material would have an index equal to one. Shell plates receive little cross-rolling and would be expected to have an anisotropy index much smaller than one. The average index for all shell plates tested at NBS [7] was found to be 0.50.

The Charpy V-notch upper shelf behavior of all head plates tested at NBS, given in Table VII, shows that the Winder plate was the least isotropic of the four head plates with an index of 0.63 compared to 0.66 for the other ASTM A212-B head plate and the average head-plate index of 0.68 (lowest index was 0.66) [7].

The minimum Charpy V-notch upper-shelf energy absorption for all specimen orientations parallel to the plate rolling plane occurs in specimens of the transverse orientation. As seen in Table VII, the transverse upper-shelf energy-absorption value for the Winder plate was lower than that of the other ASTM A212-B head plate tested, 45 ft-lbs versus 55 ft-lbs, but somewhat larger than the values of 38 ft-lbs and 40 ft-lbs for the AAR M128 head plates tested. The longitudinal upper-shelf energy-absorption values show a similar relationship for these four head plates. Thus, these results show that the upper-shelf behavior for the Winder plate is inferior to the other ASTM A212-B head plate and slightly superior to the two AAR M128 head plates.

4.9 General Discussion

The purpose of this investigation was to determine if the head plate sample taken from tank car SOEX 3033, involved in an accident near Winder, Georgia, conformed with the applicable specification for tank-car materials and to investigate the impact behavior of the plate.

Although the Winder sample satisfied most of the specification requirements for an ASTM A212-B steel, the strength requirements were not met. The results of the check chemical analysis indicated that although the Winder sample met the chemical requirements of ASTM A212-B steel, the carbon and manganese levels are well below the maximum levels permitted. At reduced levels, these two important elements often result in reduced strength properties in ferritic-pearlitic steels such as ASTM A212 steel. The observation that tensile-strength and yield-point values were below the specification minimums, while the measured percent-elongation values were well above the specification minimum, is consistent with the lower carbon and manganese content measured in this steel. The observed hardness variability is consistent with the microstructure of the Winder plate and correlates quite well with the measured tensile strength.

The Charpy V-notch ductile-to-brittle transition temperature of hot-worked carbon steels, often characterized by the 15 ft-lb transition temperature or the 50 percent shear-fracture-appearance transition temperature, is primarily determined by the steel chemistry and ferrite grain size. The ferrite grain size, as noted earlier, is strongly controlled by the prior austenite grain size which is determined by the finishing temperature and deoxidation practice and by the cooling rate through the transformation temperature. Increasing the ferrite grain size raises the transition temperature. The major influence of the steel chemistry on the transition temperature of these tank car steels results primarily from changes in the carbon and manganese levels within certain ranges. Increasing the carbon level raises the transition temperature while increasing the manganese level lowers the transition temperature.

Metallographic examination revealed the presence of a distinct microstructure consisting of Widmanstätten ferrite and a large prior austenite grain size marked by ferrite boundaries. This microstructure characterizes the two ASTM A212 head plates (Winder and Crescent City) examined at NBS to date. Differences in transition temperature behavior between the two ASTM A212-B head plates probably resulted from differences in steel chemistry and mill processing procedures. Since neither of the A212-B head plates were produced to fine-grain practice, the larger ferrite grain size of the Crescent City plate probably resulted from a higher finishing temperature. The Crescent City plate had a higher transition temperature than the Winder plate and this behavior is consistent with the larger ferrite grain size and higher level of carbon found in the Crescent City plate (see Table VIII).

Although the two AAR M128 head plates previously tested at NBS were produced to fine-grain practice, the Belle plate had a more uniform microstructure with a much finer ferrite grain size indicating a probable lower finishing temperature than the Callao plate. Although the microstructure of the Callao-head plate sample was highly variable [12], the dominant features were a coarser ferrite grain size and larger pearlite colonies compared to the Belle sample. (h) Carbon levels were the same for both plates while the Callao plate had a higher manganese level than the Belle plate. Thus the lower transition temperature for the Belle plate appears to be primarily a result of the finer ferrite grain size.

In this group of four head plates, the Crescent City plate with the largest ferrite grain size and highest carbon content had the highest transition temperature while the Belle plate with the smallest ferrite grain size, a higher manganese content and lower carbon content, had the lowest transition temperature. Based on comparisons between these four head plates of two steel types, the carbon content, the manganese content, and the ferrite grain size appear to be the most important factors influencing the Charpy V-notch transition temperature behavior.

The reportedly [1] brittle fracture appearance of the failed Winder head plate is consistent with the measured Charpy impact transition temperatures. The Winder plate has a 15 ft-lb transition temperature of 66 F. This is 26 F above the tank car service temperature at the time of the accident.

(h) The Callao head plate had an undesirable microstructure of unexpectedly high variability probably resulting from improperly controlled variables in the hot-forming process.

5. CONCLUSIONS

1. The chemical composition of the Winder plate sample, as determined by check chemical analysis, satisfied the chemical requirements of ASTM A212-B. The levels of carbon and manganese were well below the maximum permitted levels and the absence of detectable levels of aluminum or vanadium indicated that a course-grain steelmaking practice was followed.
2. The results of tensile tests indicated that the Winder sample met the minimum elongation requirement but failed to satisfy the minimum tensile-strength and yield-point requirements for ASTM A212-B steel plates.
3. The low ultimate-tensile-strength and yield-strength values and the generally observed sharp yield point in tensile tests suggests that any plastic deformation of the plate resulting from the accident was not significant and that strain aging had not occurred in this plate after the accident.
4. Ultimate-tensile-strength and yield-strength values indicate little anisotropy in the strength of the plate in the plane of the rolling direction. Tensile ductility values, measured by percent elongation, indicated that longitudinal ductility was greater than transverse ductility.
5. The results of bend tests indicated that both longitudinal and transverse specimens passed the ASTM A212-B bend requirements.
6. The results of Charpy V-notch impact tests indicated that:
 - a. The 15 ft-lb transition temperature was 26 F above the ambient temperature reported at the time of the accident.
 - b. The transition temperatures for three commonly used criteria are above 44 F and were the second highest for all of the tank-car plates tested at NBS to date.
 - c. The transition from ductile to brittle failure occurs over the same temperature range of about 200 F, from +180 F to -20 F, regardless of specimen orientation for each of the three fracture criteria.
 - d. The high impact transition temperatures for the three fracture criteria are related to the lower manganese content and the large prior austenite grain size and large ferrite grain size observed in the microstructure.

6. ACKNOWLEDGEMENT

The author wishes to express thanks to Dr. C. G. Interrante for his helpful comments, and to Mr. D. E. Harne for his excellent contributions to the metallographic, photographic, and mechanical testing portions of this report. Thanks to Mr. C. H. Brady for the grain size measurements.

CONVERSION FACTORS

$$1 \text{ ksi} = 6.89 \text{ MPa}$$

$$1 \text{ ft-lb} = 1.36 \text{ Joules}$$

$$1 \text{ mil} = 0.025 \text{ mm}$$

$$t_c^o = \frac{(t_F^o - 32)}{1.8}$$

References

- (1) Report from Inspector E. W. Timmons to Regional Director J. F. McLellen, Federal Railroad Administration, Department of Transportation, 3666 EWT-523, April 28, 1975.
- (2) Original photographs courtesy of Mr. Q. Banks, Federal Railroad Administration, Washington, D.C.
- (3) Dieter, G. E. Mechanical Metallurgy, McGraw-Hill Book Co., New York City, 1961, pp. 557-562.
- (4) Interrante, C. G., Hicho, G. E. and Harne, D. E. "A Metallurgical Analysis of Five Steel Plates Taken From A Tank Car Accident Near Crescent City, Illinois," Report No. FRA OR&D 75-48, National Bureau of Standards, March 1972, NTIS PB 250530.
- (5) Interrante, C. G. and Hicho, G. E. "Metallurgical Analysis of a Steel Plate Taken From a Tank Car Accident Near South Byron, New York," Report No. FRA OR&D 75-47, National Bureau of Standards, October 1971, NTIS PB 250063.
- (6) Interrante, C. G., Hicho, G. E. and Harne, D. E. "A Metallurgical Analysis of Eleven Steel Plates Taken From A Tank Car Accident Near Callao, Missouri," Report No. FRA OR&D 75-49, National Bureau of Standards, September 1972, NTIS PB 250544.
- (7) Interrante, C. G. "Impact Properties of Steels Taken From Four Failed Tank Cars," Report No. FRA OR&D 75-51, National Bureau of Standards, June 1976.
- (8) Rege, R. A., Forgeng, W. D. Jr., Stone, D. H. and Alger, V. V., "Microcleanliness of Steel - A New Quantitative TV Rating Method," ASTM STP 480, American Society for Testing and Materials, 1970, pp. 249-272.
- (9) Aaronson, H. I., Decomposition of Austenite by Diffusional Processes, Ed. V. F. Zackay & H. I. Aaronson, Interscience Publishers, 1962, pp. 387-545.
- (10) Atlas of Isothermal Transformation and Cooling Transformation Diagrams, American Society for Metals, 1977.
- (11) Army-Navy Approximate Hardness Tensile Strength Relationship of Carbon and Low Alloy Steels (AN-QQ-H-201).
- (12) Interrante, C. G., Early, J. G., and Hicho, G. E. "Analysis of Findings of Four Tank-Car Accident Reports," Report No. FRA OR&D 75-50, National Bureau of Standards, Jan. 1975, NTIS PB 251097.

References (continued)

- (13) Early, J. G., "Elevated-Temperature Mechanical Behavior of a Carbon-Manganese Pressure Vessel Steel," J. Engineering Materials and Technology, 99, 1977, pp. 359-365.
- (14) Eiber, R. J. and Olson, L. L., "Material Study on Steels Used in Current and Former Tank Car Construction and From Cars Involved in Accidents," AAR Report RA-03-5-33, August 21, 1975.

Table I Chemical Composition of the Winder Sample

Percent by Weight

<u>Element</u>	<u>Specification ASTM A212-65-B Ladle Analysis</u>	<u>Check Analysis</u> ^(a)
Carbon	0.31 max.	0.24
Manganese	0.90 max.	0.73
Phosphorus	0.04 max.	<0.005
Sulfur	0.05 max.	0.026
Silicon	0.13/0.33 (b)	0.26
Copper	(c)	<0.05
Nickel	(c)	<0.05
Chromium	(c)	0.07
Molybdenum	(c)	<0.05
Vanadium	(d)	<0.01
Aluminum	(d)	<0.01

(a)

Carbon was determined by combustion-conductometric analysis; all other elements were determined by emission spectroscopy.

(b)

Check analysis.

(c)

Element not specified.

(d)

Element not specified, either fine-or coarse-grain practice allowed.

Table II Tensile Properties of the Winder Sample

Specimen (a) Orientation and Code	Tensile Strength ksi	Yield Strength 0.2% Offset ksi	Yield Point ksi	Elongation Percent in one inch (b)	Reduction of Area Percent
Longitudinal - SL1	68.1	33.0	35.0	37.7	61.3
Longitudinal - SL2	67.7	33.0	33.4	37.1	61.5
Average	67.9	33.0	34.2	37.4	61.4
Transverse - ST1	67.7	32.2	34.3	35.5	56.4
Transverse - ST2	67.6	32.2	N.A.	36.0	58.0
Average	67.6	32.2	34.3	35.8	57.2
Specification	85.0 max.	(c)	38.0 min.	21	(c)
ASTM A212-B-65	70.0 min.				

(a) Although the specification ASTM A212-65 does not specify test specimen orientation, ASTM A370-73 does specify that wrought steel products are usually tested in the longitudinal direction but that where size permits and service justifies it, transverse testing is done.

(b) A comparison of elongation data obtained from different sizes of specimens of the same material can be made provided the ratio of the gage length to cross-sectional dimensions is held constant. Since the ratio of the square root of the cross-sectional area to the gage length is the same for the specimen with a 0.500-inch-diameter with a 2-inch-gage and for the specimen with a 0.250-inch-diameter with a 1-inch-gage length, the elongation data from the 1-inch-gage length specimen can be directly compared to the specification requirement based on a 2-inch-gage length.

(c) Not specified.

Table III Bend Behavior of Winder Sample

<u>Orientation</u>	<u>Ratio of Bend Diameter to Thickness d/t</u>	<u>Angle of Bend</u>	<u>Comments</u>
Longitudinal	2	180°	Passed, no evidence of crazing or cracking
Transverse	2	180°	Passed, no evidence of crazing or cracking

For all tests, $w/t = 4$.

Table IV QTM Inclusion Content Rating of Winder Sample

QTM Ratings, Inclusion Area Percent

1/4 Thickness Position (25 Fields)	Midthickness Position (50 Fields)	3/4 Thickness Position (25 Fields)	Number of Fields With Inclusion Area >0.5*	Worst Field Quarter Thickness	Midthickness
0.29	0.32	0.24	6	0.54	0.79

Effective
Magnification = X 100

* Per 100 Fields

** Per 50 Fields

Table V Drop-Weight Test Behavior of Winder Plate

<u>Specimen Code</u>	<u>Test Temperature, F</u>	<u>Comments</u>
N1	+10	Specimen cracked into two pieces
N4	+20	Starter crack propagated to both edges of specimen
N6	+30	Starter crack propagated to one edge of specimen
N8	+40	Starter crack did not propagate to either edge of specimen
N9	+40	Starter crack did not propagate to either edge of specimen

Nil-Ductility Transition Temperature = +30F

Table VI Charpy V-notch Impact Transition Temperatures
For Four Head Plate Steels Tested at NBS

Steel Type	Plate Identity	Specimen Orientation	Transition Temperature, F		
			15 ft-lbs Energy Absorption	15 mil Lateral Expansion	50 percent Shear Fracture
A212-B	Winder	Long. (LT)	66	50	111
		Trans. (TL)	67	44	100
A212-B	Crescent City ^(a) FRA-2	Long. (LT)	92	72	137
		Trans. (TL)	84	69	143
AAR M128	Callao ^(b) K-1	Long. (LT)	56	41	86
		Trans. (TL)	72	64	98
AAR M128	Belle ^(c)	Long. (LT)	-47	-43	-11
		Trans. (TL)	-49	-50	-21

(a) Reference [4]

(b) Reference [6]

(c) Reference [7]

Table VII Comparison of Charpy V-notch Upper-Shelf Behavior of Four Head Plates Tested at NBS

Steel Type	Plate Code	Upper Shelf Energy Absorption, ft-lbs		Anisotropy Index
		Longitudinal (LT)	Transverse (TL)	
A212-B	Winder	72	45	0.63
A212-B	Crescent City	81	55	0.68 (a)
AAR M128	Callao	54	38	0.70
AAR M128	Belle	68	40	0.66 (a)

(a)

The orientation of specimens from the Belle and Crescent City head plates may deviate from the true longitudinal and transverse directions. Any deviation would tend to decrease the LT upper shelf energy and increase the TL upper shelf energy, thereby resulting in an artificially higher value of the anisotropy index.

Table VIII. Comparison of Selected Results From Check Chemical Analyses of Four Head Plates Tested at NBS.

Plate Code	Steel Type	Ferrite Grain Size	Carbon	Manganese	Weight Percent Aluminum
Crescent City	A212-B	6	0.29	0.81	≤ 0.002
Winder	A212-B	7	0.24	0.73	≤ 0.01
Callao	M128	7	0.26	1.25	0.026
Belle	M128	8 1/2	0.26	1.20	(a)

(a) Not determined



Figure 1. Photograph of Tank Car SOEX 3033 at the Accident Site
Near Winder, GA.

The A-head, containing the site of impact, is shown.
Original color photograph courtesy of Q. Banks, FRA-DOT.

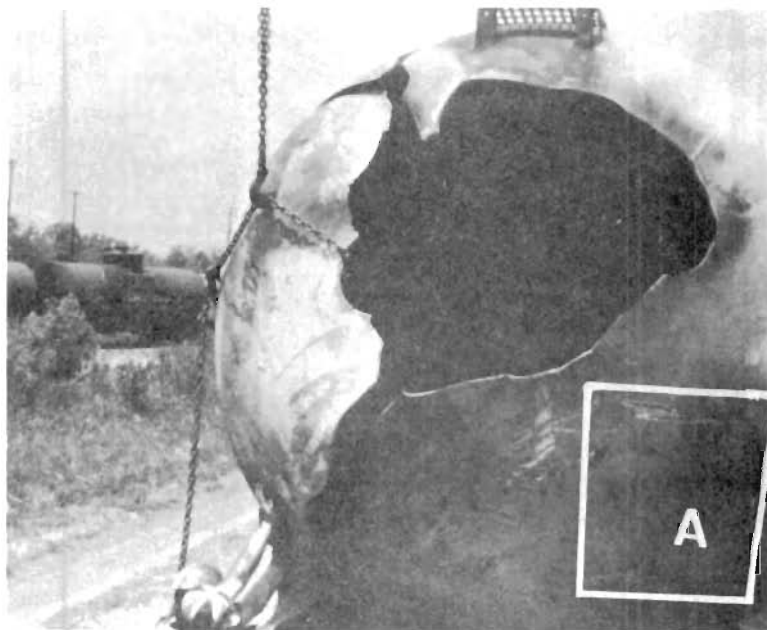


Figure 2. Close-up of A-head, Tank Car SOEX 3033.

The plate sample submitted to NBS for study was taken from a relatively undamaged region, shown at A.



Figure 3. Winder Plate Sample.

Principal plate rolling direction determined with respect to an arbitrary reference line scribed on the plate surface, marked as REF. Chemistry and metallographic samples were taken from locations marked CHEM and MET, respectively.

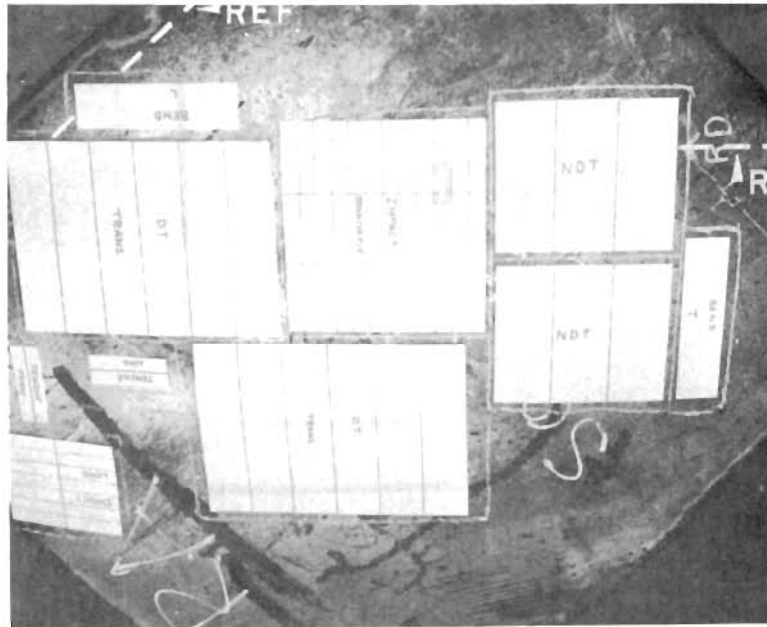


Figure 4. Winder Plate Sample Showing Location and Orientation of Test Specimens.

Principal rolling direction of the plate and arbitrary reference line are shown marked as RD and REF, respectively.

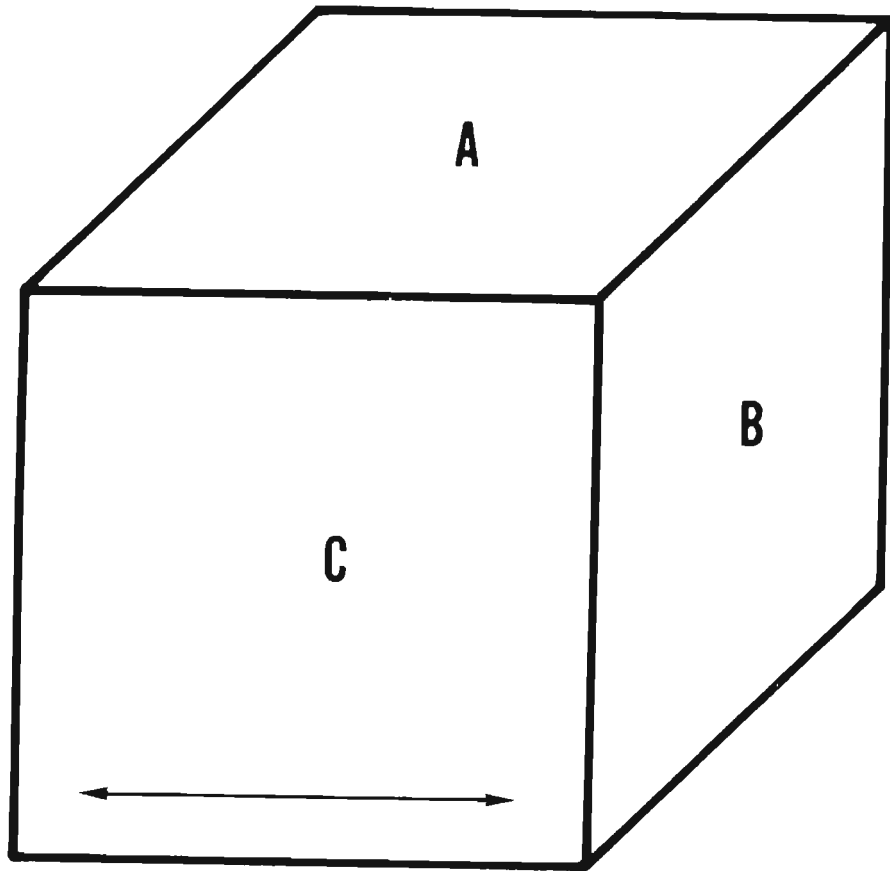


Figure 5. Schematic Showing the Three Mutually Perpendicular Planes Associated with the Rolling Direction in a Plate. The A plane is parallel to the plate surface. The C plane contains an arrow which indicates the plate rolling direction or longitudinal direction.



Figure 6. Representative Photomicrographs of Inclusions on Two Orthogonal Planes

- a. Longitudinal or C plane
- b. Transverse or B plane

Unetched

Mag. X 100

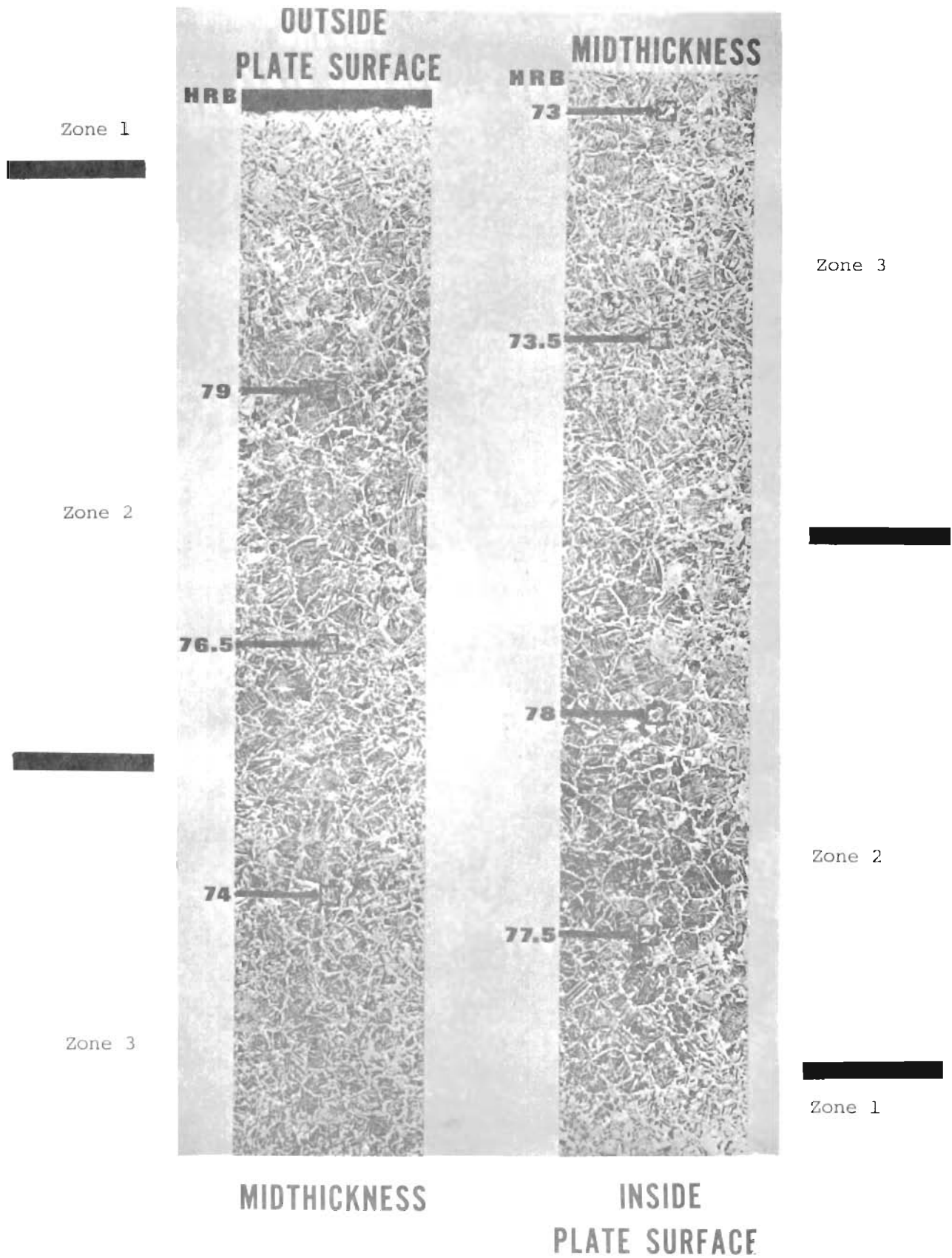
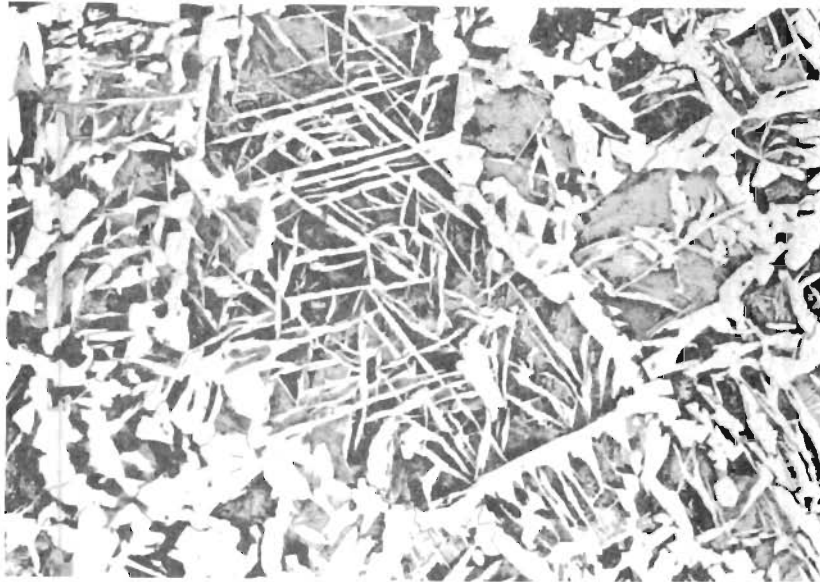


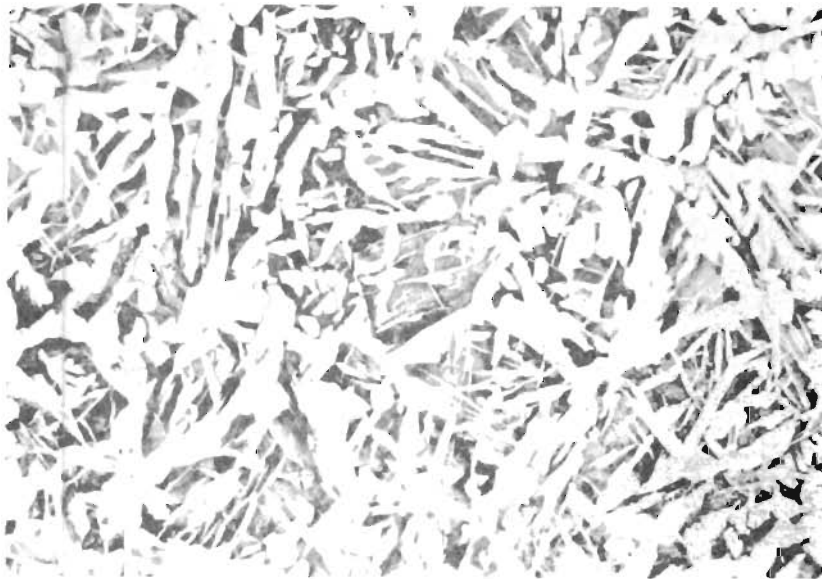
Figure 7. Montage of Microstructure Through Cross-Section of the Plate. Hardness values are representative of the locations shown.

Etch: 5% Nital

Original Micrographs Mag. X 40



a.



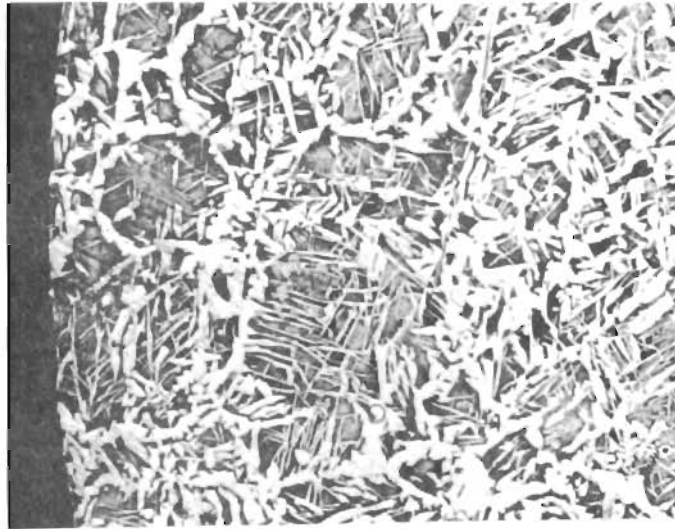
b.

Figure 8. Photomicrographs of Typical Microstructure from Zones 2 and 3.

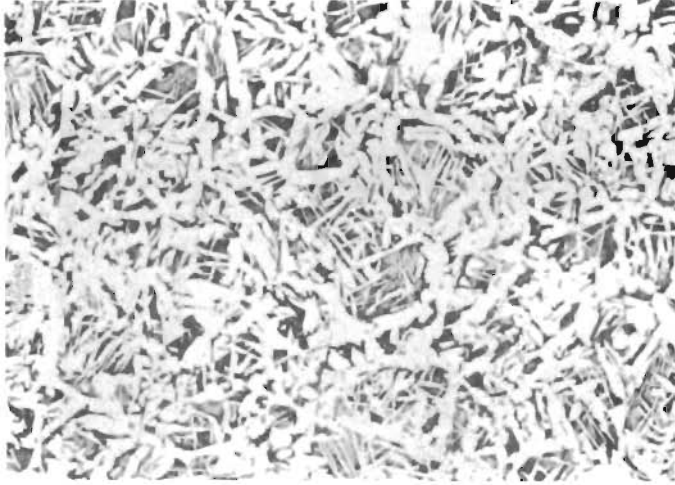
- a. Zone 2 Pearlite colonies, surrounded by ferrite grains on prior austenite grain boundaries, containing Widmanstätten ferrite.
- b. Zone 3 Large amounts of ferrite mask prior austenite grain boundaries. Widmanstätten ferrite has greatly thickened.

Etch: 4% Picral

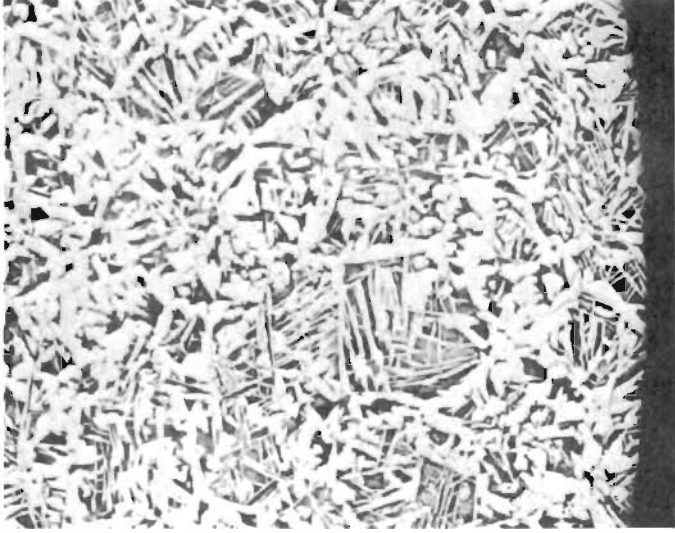
Mag. X 100



a. Tensile specimen shoulder,
near plate surface



b. Gage length region

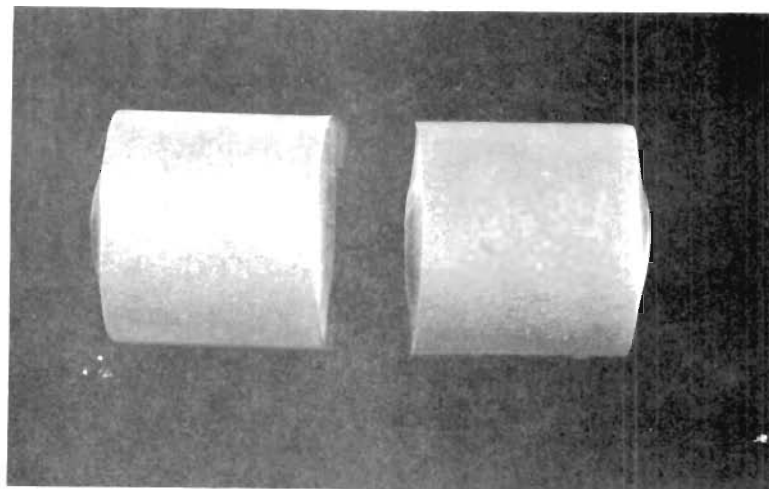


c. Tensile specimen shoulder,
near plate midthickness
region

Figure 9. Representative Photomicrographs of a Section Through a Transverse
Tensile Specimen Showing the Longitudinal or C Plane

Etch: 4% Picral

Mag. X 40



a.

b.

Figure 10. Bend Test Specimens

a. Longitudinal specimen

b. Transverse specimen

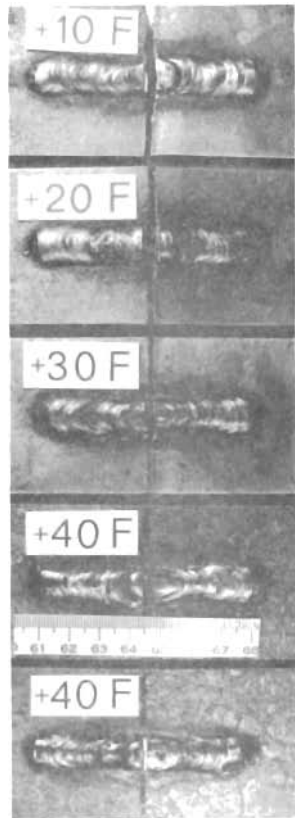


Figure 11. Drop-Weight Test Specimens.
Nil-Ductility Transition Temperature (NDT
temperature) = +30 F

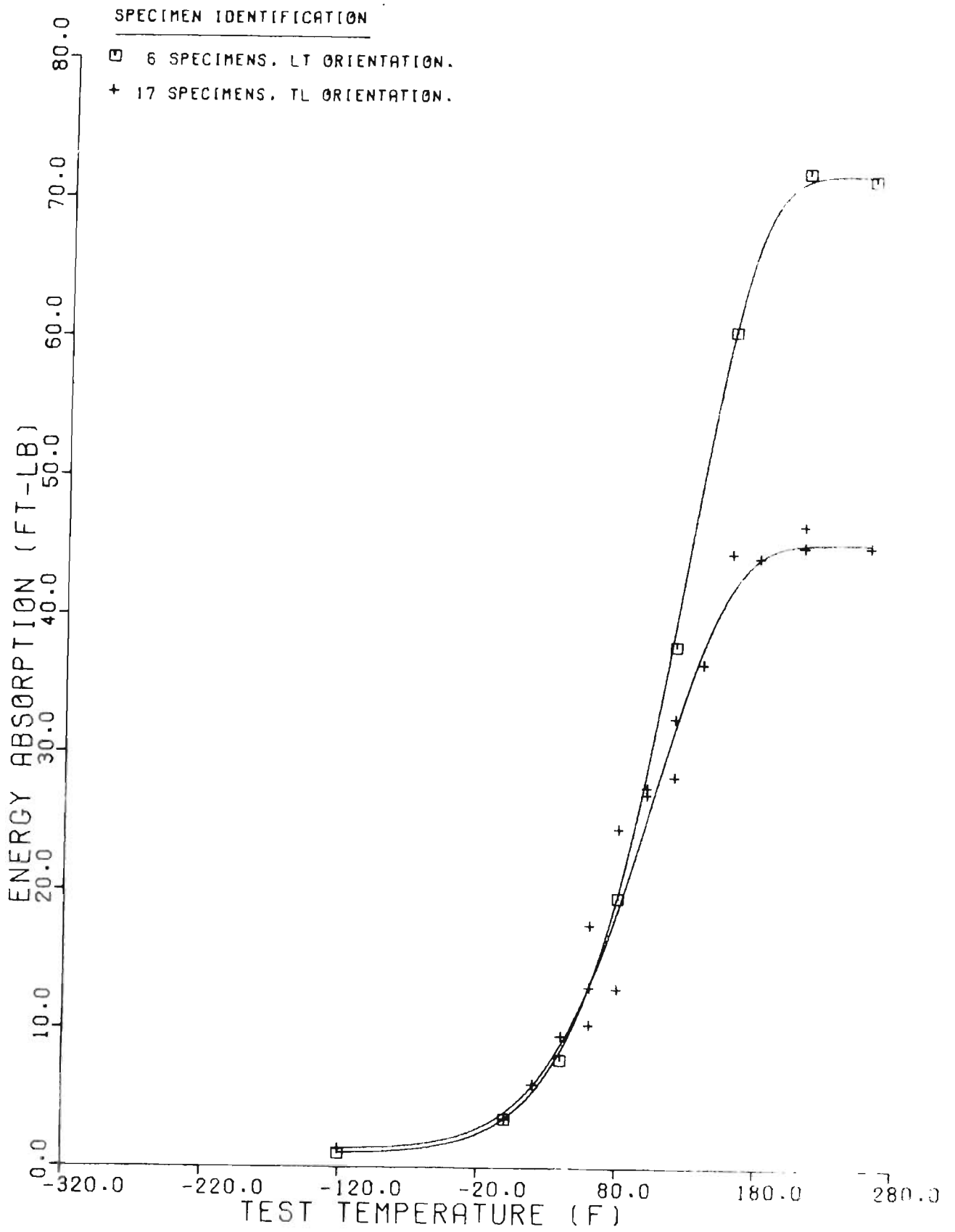


Figure 12a.

CHARPY IMPACT TEST RESULTS FOR HEAD PLATE SPECIMENS
 TAKEN FROM ASTM A212 STEEL PLATE S

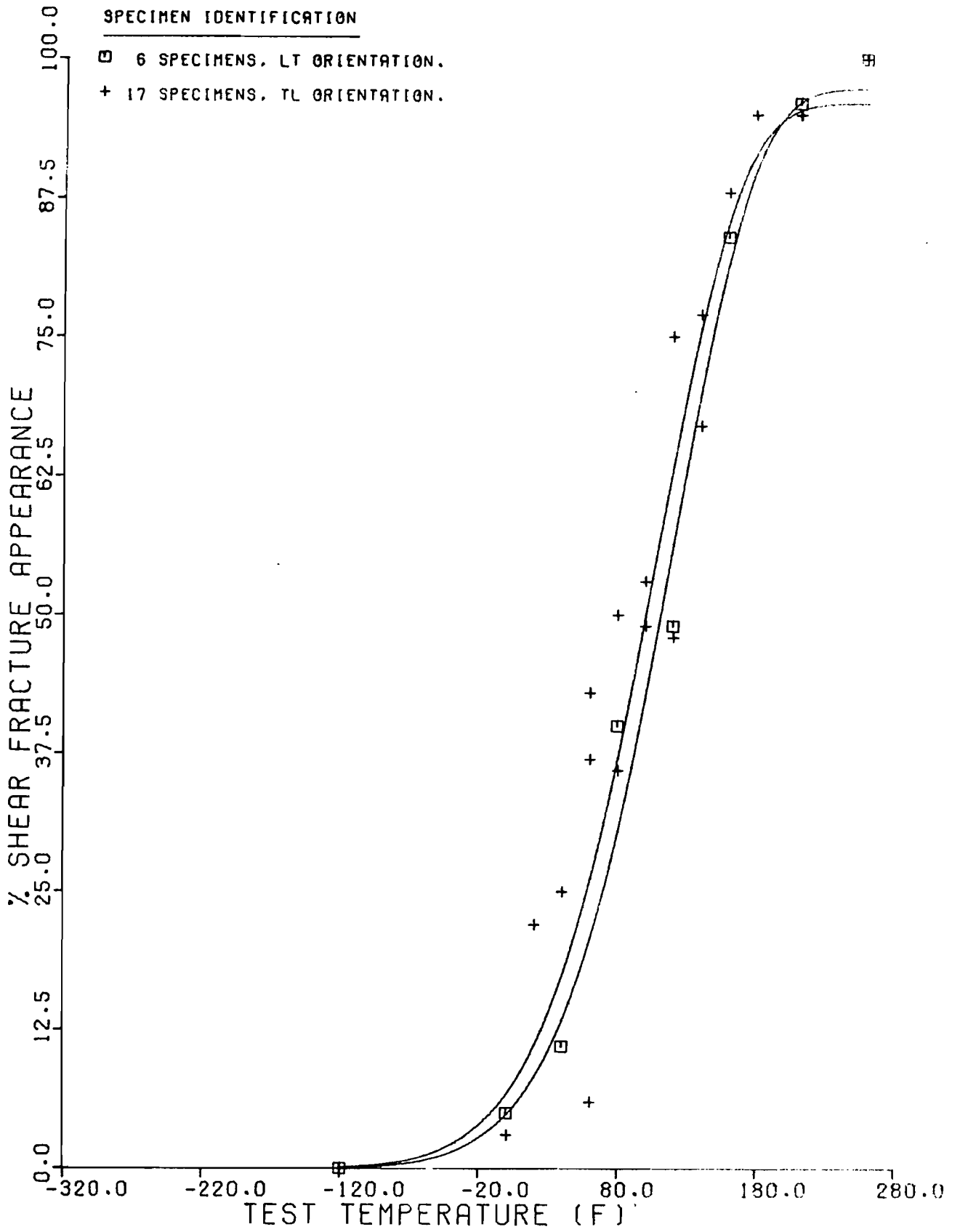


Figure 12b. CHARPY IMPACT TEST RESULTS FOR HEAD PLATE SPECIMENS TAKEN FROM ASTM A212 STEEL PLATE S

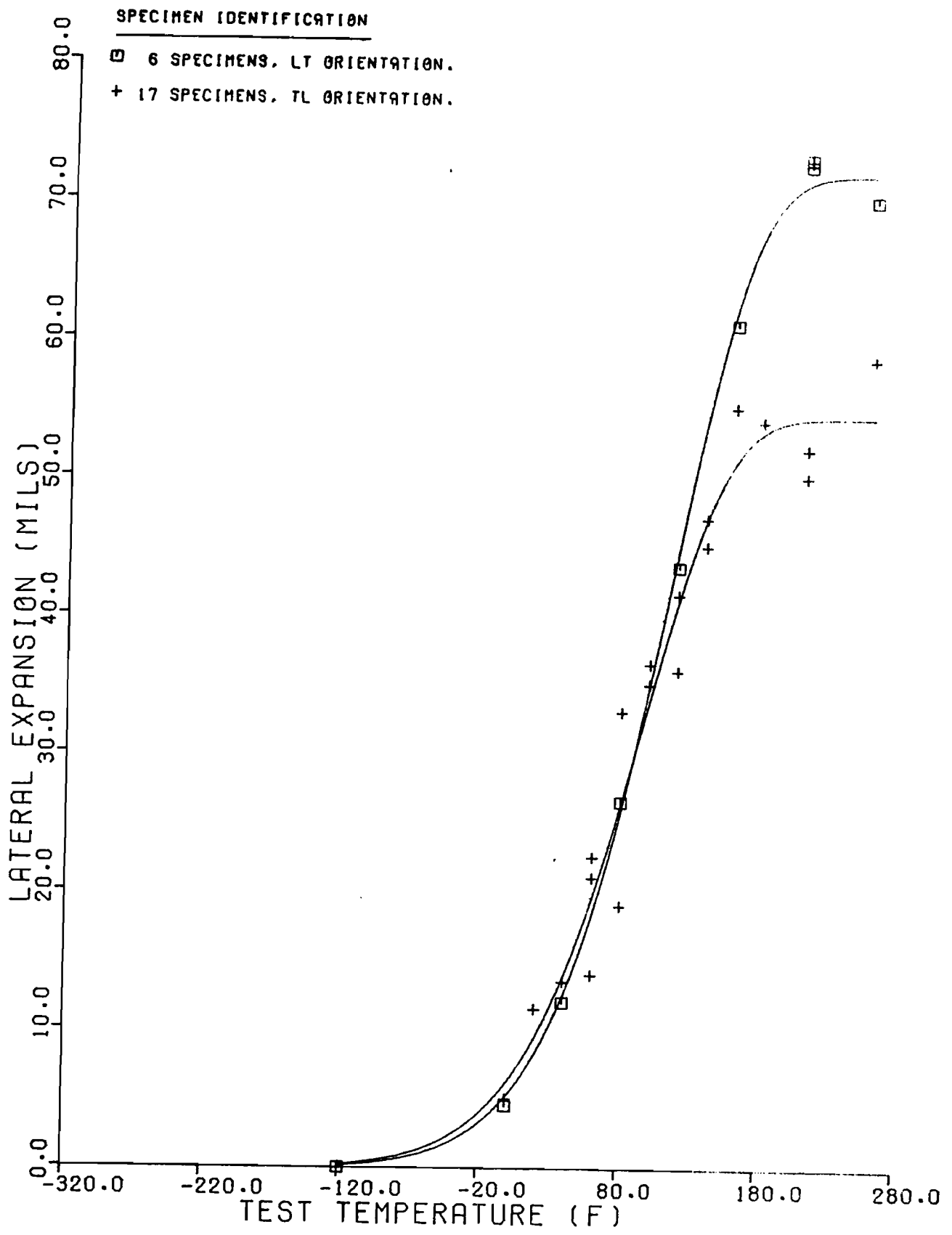


Figure 12c. CHARPY IMPACT TEST RESULTS FOR HEAD PLATE SPECIMENS TAKEN FROM ASTM A212 STEEL PLATE S


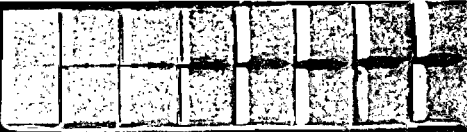

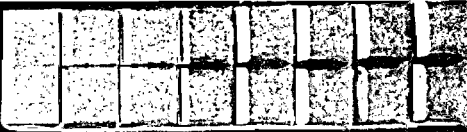

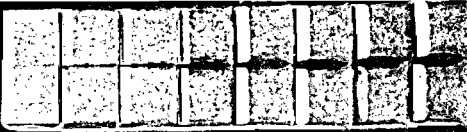

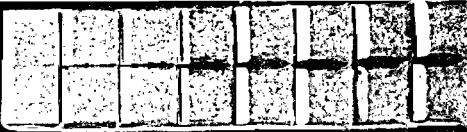

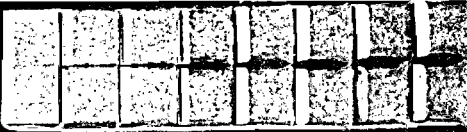

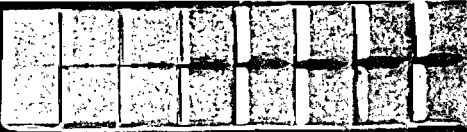

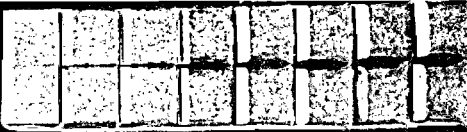

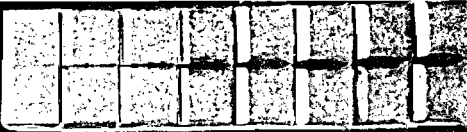

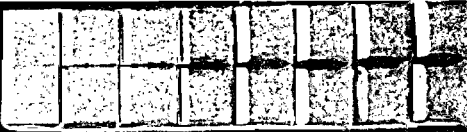

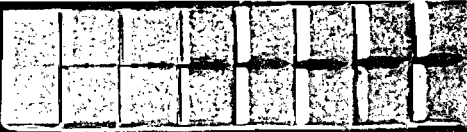

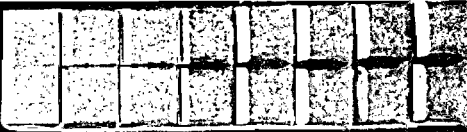

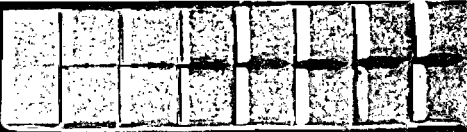
Sample No.	Energy Abs. (ft-lb)	Test Temperature	Fracture Appearance		Sample No.
			Transverse	Longitudinal	
ST22	1	-120 F			SL4
ST18	3 1/2	0 F			SL10
ST19	9 1/2	40 F			SL7
ST15	13	60 F			SL14
ST26	24 1/2	80 F			SL11
ST32	27	100 F			SL13
ST35	28	120 F			SL40
ST34	36	140 F			SL6
ST28	44 1/2	160 F			
ST7	44	180 F			
T3	45	212 F			
ST31	45	260 F			

Figure 13. Fracture Appearance of Selected Charpy Specimens Taken from the Winder Sample.



Appendix A, Table A1

CHARPY IMPACT TEST RESULTS FOR HEAD PLATE SPECIMENS
TAKEN FROM ASTM A212 STEEL PLATE S

CALCULATIONS FOR ENERGY ABSORPTION DATA OF
6 SPECIMENS, LT ORIENTATION.

SPECIMEN	TEMPERATURE(F)	OBSERVED ENERGY ABSORPTION(FT-LB)	CALCULATED ENERGY ABSORPTION(FT-LB)
SL4	-120.0	1.00	1.0
SL10	.0	3.50	3.6
SL7	40.0	7.80	8.5
SL14	80.0	19.50	19.9
SL11	120.0	37.80	39.5
SL13	160.0	60.50	60.8
40-1	212.0	72.00	71.4
40-2	212.0	72.00	71.4
SL6	260.0	71.50	71.8

TRANSITION REGION. CALCULATED VALUES

ENERGY ABSORPTION	CALCULATED TEMPERATURE(F)	/	TEMPERATURE (F)	CALCULATED ENERGY ABSORPTION(FT-LB)
5.0	15.9	/	20.0	5.5
10.0	47.3	/	25.0	6.1
15.0	66.2	/	30.0	6.8
20.0	80.4	/	35.0	7.6
25.0	92.1	/	40.0	8.5
30.0	102.4	/	45.0	9.5
35.0	111.9	/	50.0	10.6
40.0	120.8	/	55.0	11.8
45.0	129.6	/	60.0	13.2
50.0	138.5	/	65.0	14.6
55.0	147.8	/	70.0	16.2
60.0	158.3	/	75.0	18.0
65.0	171.3	/	80.0	19.9
70.0	193.8	/	85.0	21.9
		/	90.0	24.0
		/	95.0	26.3
		/	100.0	28.8
		/	105.0	31.3
		/	110.0	34.0
		/	115.0	36.7

Appendix A, Table A2

CHARPY IMPACT TEST RESULTS FOR HEAD PLATE SPECIMENS
TAKEN FROM ASTM A212 STEEL PLATE S

CALCULATIONS FOR LATERAL EXPANSION DATA OF
6 SPECIMENS, LT ORIENTATION.

SPECIMEN	TEMPERATURE (F)	OBSERVED LATERAL EXPANSION (MILS)	CALCULATED LATERAL EXPANSION (MILS)
SL4	-120.0	.00	.2
SL10	.0	4.50	5.1
SL7	40.0	12.00	12.4
SL14	80.0	26.50	25.8
SL11	120.0	43.50	44.7
SL13	160.0	61.00	62.2
40-1	212.0	72.50	71.2
40-2	212.0	73.00	71.2
SL6	260.0	70.00	71.8

TRANSITION REGION, CALCULATED VALUES

LATERAL EXPANSION(MILS)	CALCULATED TEMPERATURE(F)	/	TEMPERATURE (F)	CALCULATED LATERAL EXPANSION(MILS)
5.0	-1.1	/	.0	5.1
10.0	29.6	/	5.0	5.8
15.0	49.6	/	10.0	6.5
20.0	65.0	/	15.0	7.3
25.0	78.1	/	20.0	8.1
30.0	89.6	/	25.0	9.1
35.0	100.3	/	30.0	10.1
40.0	110.5	/	35.0	11.2
45.0	120.6	/	40.0	12.4
50.0	130.8	/	45.0	13.7
55.0	141.6	/	50.0	15.1
60.0	153.8	/	55.0	16.6
65.0	169.1	/	60.0	18.3
70.0	195.7	/	65.0	20.0
		/	70.0	21.8
		/	75.0	23.8
		/	80.0	25.8
		/	85.0	27.9
		/	90.0	30.2
		/	95.0	32.5

Appendix A, Table A3

CHARPY IMPACT TEST RESULTS FOR HEAD PLATE SPECIMENS
TAKEN FROM ASTM A212 STEEL PLATE S

CALCULATIONS FOR SHEAR FRACTURE APPEARANCE DATA OF
6 SPECIMENS, LT ORIENTATION.

SPECIMEN	TEMPERATURE (F)	OBSERVED SHEAR FRACTURE (%)	CALCULATED SHEAR FRACTURE (%)
SL4	-120.0	.00	.1
SL10	.0	5.00	4.9
SL7	40.0	11.00	13.4
SL14	80.0	40.00	30.5
SL11	120.0	49.00	56.3
SL13	160.0	84.00	81.7
40-1	212.0	96.00	96.1
40-2	212.0	96.00	96.1
SL6	260.0	100.00	97.3

TRANSITION REGION, CALCULATED VALUES

% SHEAR FRACTURE	CALCULATED TEMPERATURE (F)	/	TEMPERATURE (F)	CALCULATED SHEAR FRACTURE (%)
2.0	-29.9	/	-20.0	2.7
5.0	1.1	/	-10.0	3.7
10.0	27.7	/	.0	4.9
15.0	45.1	/	10.0	6.4
50.0	111.0	/	20.0	8.2
85.0	166.9	/	30.0	10.6
90.0	179.9	/	40.0	13.4
95.0	201.9	/	50.0	16.7
98.0	260.0	/	60.0	20.7
		/	70.0	25.3
		/	80.0	30.5
		/	90.0	36.3
		/	100.0	42.5
		/	110.0	49.3
		/	120.0	56.3
		/	130.0	63.2
		/	140.0	69.9
		/	150.0	76.2
		/	160.0	81.7
		/	170.0	86.3

Appendix A, Table A4

CHARPY IMPACT TEST RESULTS FOR HEAD PLATE SPECIMENS
 TAKEN FROM ASTM A212 STEEL PLATE S
 CALCULATIONS FOR ENERGY ABSORPTION DATA OF
 17 SPECIMENS, TL ORIENTATION.

SPECIMEN	TEMPERATURE(F)	OBSERVED ENERGY ABSORPTION(FT-LB)	CALCULATED ENERGY ABSORPTION(FT-LB)
ST22	-120.0	1.30	1.3
ST18	.0	3.50	4.0
ST25	20.0	6.00	5.9
ST19	40.0	9.50	8.9
ST1	60.0	17.50	13.1
ST15	60.0	13.00	13.1
ST36	60.0	10.30	13.1
ST27	80.0	12.90	13.6
ST26	80.0	24.50	13.6
ST32	100.0	27.00	25.1
ST6	100.0	27.50	25.1
ST35	120.0	28.30	31.8
ST33	120.0	32.50	31.8
ST11	140.0	36.50	37.7
ST34	140.0	36.50	37.7
ST28	160.0	44.50	41.8
ST7	180.0	44.20	44.1
T-2	212.0	45.00	45.1
T-3	212.0	45.00	45.1
T-4	212.0	46.50	45.1
ST31	260.0	45.00	45.2

TRANSITION REGION, CALCULATED VALUES

ENERGY ABSORPTION	CALCULATED TEMPERATURE(F)	/	TEMPERATURE (F)	CALCULATED ENERGY ABSORPTION(FT-LB)
5.0	11.7	/	20.0	5.9
10.0	45.9	/	25.0	6.6
15.0	67.4	/	30.0	7.3
20.0	84.5	/	35.0	8.0
25.0	99.8	/	40.0	8.9
30.0	114.6	/	45.0	9.8
35.0	130.4	/	50.0	10.8
40.0	150.0	/	55.0	11.9
45.0	202.4	/	60.0	13.1
		/	65.0	14.4
		/	70.0	15.7
		/	75.0	17.1
		/	80.0	18.5
		/	85.0	20.2
		/	90.0	21.8
		/	95.0	23.4
		/	100.0	25.1
		/	105.0	26.8
		/	110.0	28.5
		/	115.0	30.1

Appendix A, Table A5

CHARPY IMPACT TEST RESULTS FOR HEAD PLATE SPECIMENS
 TAKEN FROM ASTM A212 STEEL PLATE S
 CALCULATIONS FOR LATERAL EXPANSION DATA OF
 17 SPECIMENS, TL ORIENTATION.

SPECIMEN	TEMPERATURE (F)	OBSERVED LATERAL EXPANSION (MILS)	CALCULATED LATERAL EXPANSION (MILS)
ST22	-120.0	.00	.2
ST18	.0	5.00	6.1
ST25	20.0	11.50	9.4
ST19	40.0	13.50	13.8
ST1	60.0	22.50	19.5
ST15	60.0	21.00	19.5
ST36	60.0	14.00	19.5
ST27	80.0	19.00	26.4
ST26	80.0	33.00	26.4
ST32	100.0	36.50	33.8
ST6	100.0	35.00	33.8
ST35	120.0	36.00	41.0
ST33	120.0	41.50	41.0
ST11	140.0	45.00	47.0
ST34	140.0	47.00	47.0
ST28	160.0	55.00	51.0
ST7	180.0	54.00	53.2
T-2	212.0	52.00	54.2
T-3	212.0	52.00	54.2
T-4	212.0	50.00	54.2
ST31	260.0	58.50	54.3

TRANSITION REGION, CALCULATED VALUES

LATERAL EXPANSION (MILS)	CALCULATED TEMPERATURE (F)	/	TEMPERATURE (F)	CALCULATED LATERAL EXPANSION (MILS)
5.0	-8.9	/	.0	6.1
10.0	23.2	/	5.0	6.8
15.0	44.5	/	10.0	7.6
20.0	61.5	/	15.0	8.5
25.0	76.2	/	20.0	9.4
30.0	89.8	/	25.0	10.4
35.0	103.2	/	30.0	11.4
40.0	117.1	/	35.0	12.6
45.0	132.7	/	40.0	13.8
50.0	153.8	/	45.0	15.1
		/	50.0	16.5
		/	55.0	18.0
		/	60.0	19.5
		/	65.0	21.1
		/	70.0	22.8
		/	75.0	24.6
		/	80.0	26.4
		/	85.0	28.2
		/	90.0	30.1
		/	95.0	31.9

Appendix A, Table A6

CHARPY IMPACT TEST RESULTS FOR HEAD PLATE SPECIMENS
 TAKEN FROM ASTM A212 STEEL PLATE S
 CALCULATIONS FOR SHEAR FRACTURE APPEARANCE DATA OF
 17 SPECIMENS, TL ORIENTATION.

SPECIMEN	TEMPERATURE (F)	OBSERVED SHEAR FRACTURE (%)	CALCULATED SHEAR FRACTURE (%)
ST22	-120.0	.00	.1
ST18	.0	3.00	0.7
ST25	20.0	22.00	11.1
ST19	40.0	25.00	17.5
ST1	60.0	43.00	26.1
ST15	60.0	37.00	26.1
ST36	60.0	6.00	26.1
ST27	80.0	36.00	37.1
ST26	80.0	50.00	37.1
ST32	100.0	49.00	49.9
ST6	100.0	53.00	49.9
ST35	120.0	48.00	63.4
ST33	120.0	75.00	63.4
ST11	140.0	77.00	75.7
ST34	140.0	67.00	75.7
ST28	160.0	88.00	85.4
ST7	180.0	95.00	91.5
T-2	212.0	95.00	95.4
T-3	212.0	95.00	95.4
T-4	212.0	95.00	95.4
ST31	260.0	100.00	95.0

TRANSITION REGION. CALCULATED VALUES

% SHEAR FRACTURE	CALCULATED TEMPERATURE (F)	/	TEMPERATURE (F)	CALCULATED SHEAR FRACTURE (%)
2.0	-41.9	/	-40.0	2.1
5.0	-11.1	/	-25.0	3.4
10.0	15.6	/	-10.0	5.2
15.0	33.0	/	5.0	7.7
50.0	100.1	/	20.0	11.1
85.0	159.1	/	35.0	15.7
90.0	173.8	/	50.0	21.5
95.0	205.2	/	65.0	28.7
98.0	260.0	/	80.0	37.1
		/	95.0	46.6
		/	110.0	56.7
		/	125.0	66.6
		/	140.0	75.7
		/	155.0	83.3
		/	170.0	88.9
		/	185.0	92.5
		/	200.0	94.6
		/	215.0	95.5
		/	230.0	95.9
		/	245.0	96.0

